JACS
JOURNAL OF THE AMERICAN CHEMICAL SOCIETY

ARTICLE

pubs.acs.org/JACS

[2 + 2] Cycloaddition Reaction to $Sc_3N@I_h$-C_{80}. The Formation of Very Stable [5,6]- and [6,6]-Adducts

Fang-Fang Li,[†] Julio R. Pinzón,[‡] Brandon Q. Mercado,[§] Marilyn M. Olmstead,*[,§] Alan L. Balch,*[,§] and Luis Echegoyen*[,†]

[†]Department of Chemistry, University of Texas at El Paso, El Paso, Texas 79968, United States

[‡]Department of Chemistry, Clemson University, Clemson, South Carolina 29634, United States

[§]Department of Chemistry, University of California at Davis, Davis, California 95616, United States

Supporting Information

ABSTRACT: The [2 + 2] cycloaddition reaction of $Sc_3N@I_h$-C_{80} with benzyne was successfully conducted for the first time. The reaction affords both the [5,6]- and [6,6]-monoadducts with a four-membered ring attached to the cage surface on 5,6- and 6,6-ring fusions, respectively. The compounds were characterized by MALDI-TOF, NMR, UV−vis−NIR spectroscopy and single-crystal X-ray structure determination. The electrochemical behavior of both monoadducts was investigated. The [5,6]-regioisomer displays reversible cathodic behavior similar to that observed for the fulleropyrrolidines with a 5,6-addition pattern. Surprisingly, the [6,6]-regioisomer also exhibits reversible cathodic behavior. The interconversion reaction of the isomers was also explored, and the results showed that both monoadducts are thermally very stable.

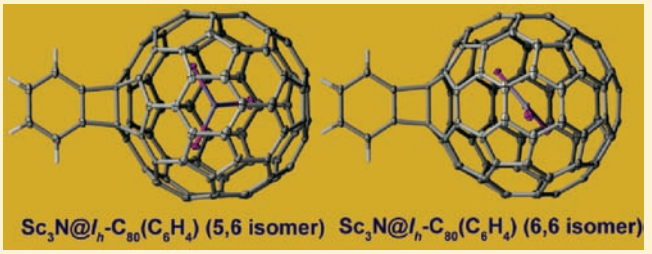

INTRODUCTION

Trimetallic nitride template endohedral metallofullerenes (TNT-EMFs)[1−4] have attracted considerable attention from the scientific community due to their promising applications in many fields, such as biomedicine,[5−10] organic solar cell,[11−16] and nanomaterials science.[4] Exohedral chemical functionalization of TNT-EMFs is crucial in the development of novel organometallofullerene materials for a variety of potential applications. In order to functionalize TNT-EMFs, those reactions that have been successful with empty-cage fullerenes have been applied to various TNT-EMFs. The first reported derivative was a Diels−Alder adduct of $Sc_3N@I_h$-C_{80}, which formed with high regioselectivity on a [5,6]-bond (bond located between a five- and a six-membered ring).[17,18] Later the 1,3-dipolar cycloaddition of azomethine ylides[19] was reported.[20,21] For this reaction, the regioselectivity of the addition is controlled by the encapsulated metal.[22−26] In the case of $Sc_3N@I_h$-C_{80} the [5,6]-pyrrolidine is the preferred isomer, whereas for larger metals the [6,6]-isomer seems to be preferentially formed. In fact, the only reported example of the simultaneous formation of both the [5,6]- and the [6,6]-$Sc_3N@I_h$-C_{80} fulleropyrrolidines occurred when $Sc_3N@I_h$-C_{80} was reacted with *N*-trityloxazolidinone but the *N*-trityl-[6,6]-$Sc_3N@I_h$-C_{80} fulleropyrrolidine isomerizes to the corresponding [5,6]-regioisomer upon heating.[27] Identical behavior has been observed for the fulleropyrrolidine derivatives of $M_3N@I_h$-C_{80} except for $Gd_3N@I_h$-C_{80},[25] indicating that the [6,6]-regioisomer is a kinetic product, whereas the [5,6]-regioisomer is the thermodynamic product.

The free radical addition of 1,1,2,2-tetramesityl-1,2-disilirane to $Sc_3N@I_h$-C_{80} produced both the 1,2 addition product on a [5,6]-bond and the 1,4-addition product with high regioselectivity.[28,29] This reaction proceeded only under UV irradiation, and the 1,2-addition product isomerized to the 1,4-product upon heating. Similarly, the free radical trifluoromethylation[30] and the reaction with benzyl bromide under UV irradiation produced identical 1,4 addition patterns.[31] The Bingel−Hirsch reaction[32,33] on TNT-EMFs occurred regioselectively on a 6,6-ring junction[22,23,34−37] and produced open-cage fulleroid derivatives. The addition of diazoalkanes to TNT-EMFs with I_h-C_{80} cages also produced [6,6]-open fulleroid derivatives.[14]

The electrochemical properties of TNT-EMF derivatives are potentially useful in molecular electronics and in solar cell construction. For example, the very negative potential of some TNT-EMF derivatives can lead to higher open circuit voltage devices and hence to improved efficiencies.[15,16,35] The [5,6]-$M_3N@I_h$-C_{80} fulleropyrrolidines (M = Sc, Y, Er) have reversible reductive electrochemical behavior,[23] whereas the [6,6]-$M_3N@I_h$-C_{80} fulleropyrrolidines (M = Y, Er) and the [6,6]-$M_3N@I_h$-C_{80} (M = Lu, Sc, Er, Y) open-cage fulleroids[14,22,23,34−37] exhibit irreversible reductive behavior similar to that of the pristine fullerene cages.[23]

The study of the reaction between benzyne and fullerenes began in 1992 when two groups reported the formation of mono-,

Received: October 28, 2010
Published: January 10, 2011

   dx.doi.org/10.1021/ja1097176 | *J. Am. Chem. Soc.* 2011, 133, 1563–1571

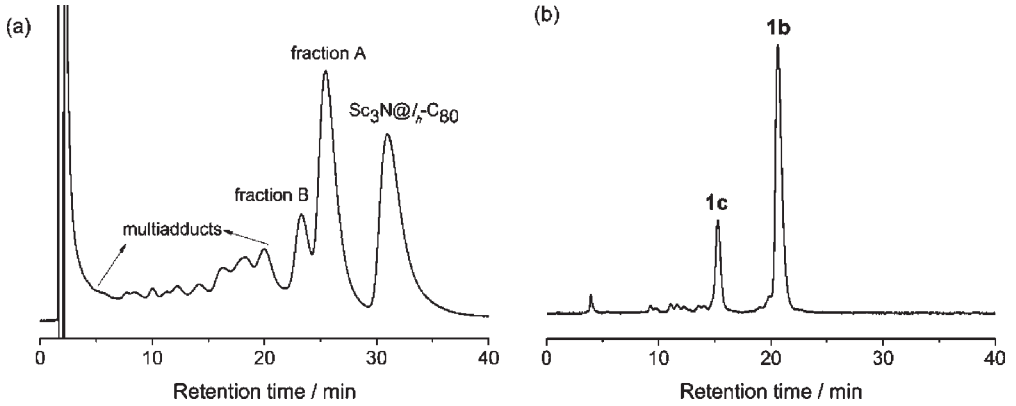

Figure 1. (a) HPLC profile of reaction mixtures. Conditions: column, PBB; eluent, toluene 2 mL/min; (b) HPLC profile of fraction B isolated from PBB. Conditions: column, Buckyprep; eluent, toluene 4 mL/min.

di-, tri-, and tetra-adducts of benzyne and C_{60}.[38,39] Subsequently, the monoadduct of C_{60} and 4,5-dimethoxybenzyne was examined crystallographically.[40] Addition occurred at a 6,6-ring junction and resulted in the elongation of the fullerene C−C bond from 1.38 Å to 1.645(8) Å. Addition of benzyne to C_{70} produced four monoadducts.[41] In three of these products, the addition occurred at a 6,6-ring junction. In the major product, which has been crystallographically characterized, addition occurred at the most pyramidalized carbon atoms (C1 and C2) at the pole of the molecule. However, ^{13}C NMR studies indicate that the least abundant adduct involves addition to a 5,6-ring junction. Benzyne has also been successfully added to endohedral fullerenes. The reaction between $Gd@C_{82}$ and benzyne produced both [5,6]- and [6,6]-monoadducts.[42] Treatment of $La@C_{82}$ with anthranilic acid and isoamyl nitrite produced $La@C_{82}$-$(C_6H_4)_2NO_2$, which has been characterized by single-crystal X-ray diffraction.[43] In this adduct both benzyne units have added across 5,6-ring junctions of the carbon cage to form closed cyclobutenyl units. The synthesis, characterization, regioselectivity of addition, and properties of adducts resulting from [2 + 2] cycloaddition reactions of TNT-EMFs have not been investigated previously. In this contribution we report that the addition of benzyne to the $Sc_3N@I_h$-C_{80} cage results in the formation of two, very stable, isomeric monoadducts.

RESULTS AND DISCUSSION

Preparation and Purification of $Sc_3N@I_h$-C_{80}. The soot containing scandium metallofullerenes was prepared according to the reported procedure using a composite anode which contained graphite, scandium oxide, and copper with the weight ratio of $C/Sc_2O_3/Cu$ equal to 7/2/1.[44] The composite rod was annealed at 1000 °C for 12 h and subjected to an arc discharge as an anode in a helium atmosphere (200 Torr) that contained a small amount of NH_3 gas (10 Torr). The raw soot containing scandium metallofullerenes was collected and extracted with CS_2 for 3 h. The fullerenes were isolated from polyaromatic hydrocarbons by flash chromatography on silica eluting with CS_2. The first fraction containing the fullerenes was collected, and the solvent was evaporated. The remaining black solid was washed with diethyl ether and dichloromethane in order to remove remaining empty cage fullerenes. Finally, $Sc_3N@I_h$-C_{80} was purified by selective chemical oxidation with tris(*p*-bromophenyl)aminium hexachloroantimonate (TBAPH) which removes

Scheme 1. [2 + 2] Cycloaddition Reaction to $Sc_3N@I_h$-C_{80}

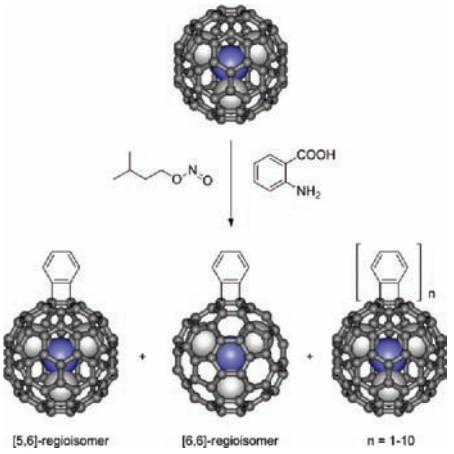

the $Sc_3N@D_{5h}$-C_{80}, $Sc_3N@D_{3h}$-C_{78}, and $Sc_3N@D_3$-C_{68} that are present in the fullerene mixture.[45]

[2 + 2] Cycloaddition Reaction on $Sc_3N@I_h$-C_{80}: Synthesis and Purification of Adducts. Procedures for the generation of both isomers are similar to those reported previously.[43] *o*-Dichlorobenzene and toluene solution containing $Sc_3N@I_h$-C_{80} was bubbled with argon for 10 min, and 15 equiv of isoamyl nitrite was added with argon bubbling for another 10 min, and then 15 equiv of anthranilic acid was added. After stirring under argon for 3 h at room temperature, compounds **1a** and **1b** with the respective yield of 70% and 15% based on consumed $Sc_3N@I_h$-C_{80} were isolated from the reaction mixtures and purified through two HPLC stages with toluene as solvent. Details of the synthesis are shown in Scheme 1 and described in the Experimental Section. The reaction mixtures in toluene were initially separated using a PBB column to isolate fractions A and B and to recover the unreacted $Sc_3N@I_h$-C_{80} as shown in Figure 1a. Further chromatography using a Buckyprep column revealed that fraction A contained only compound **1a**, while fraction B contained two compounds, **1b** and **1c** (Figure 1b). **1a** and **1b** are assigned as benzyne monoadducts of $Sc_3N@I_h$-C_{80}. **1c** with the yield of 5% based on consumed $Sc_3N@I_h$-C_{80} corresponds to a benzyne bis-adduct of $Sc_3N@I_h$-C_{80} based on the MALDI-TOF mass value.

dx.doi.org/10.1021/ja1097176 |*J. Am. Chem. Soc.* 2011, 133, 1563–1571

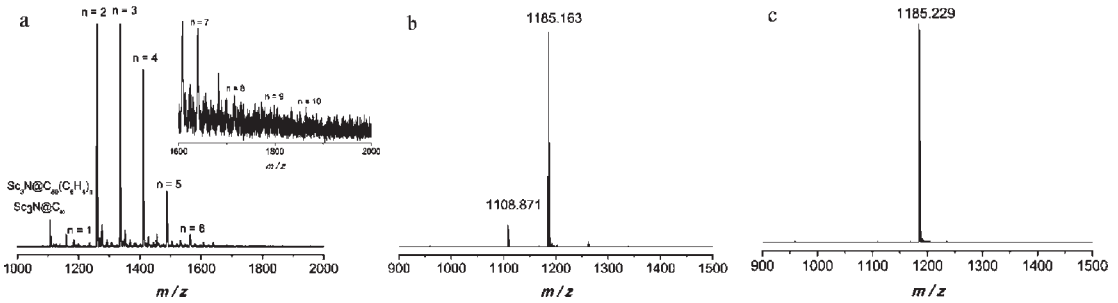

Figure 2. MALDI TOF mass spectra of multiple adducts (a), **1a** (b), and **1b** (c).

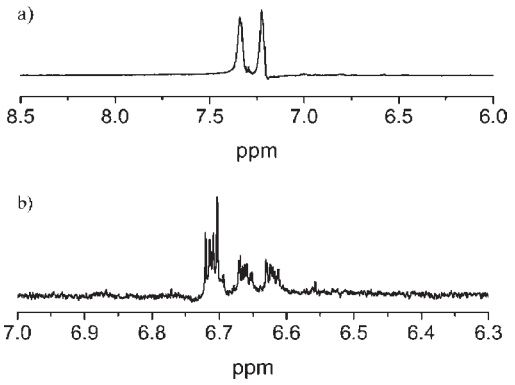

Figure 3. Proton NMR spectra of (a) **1a** and (b) **1b** in CS_2/CD_3COCD_3.

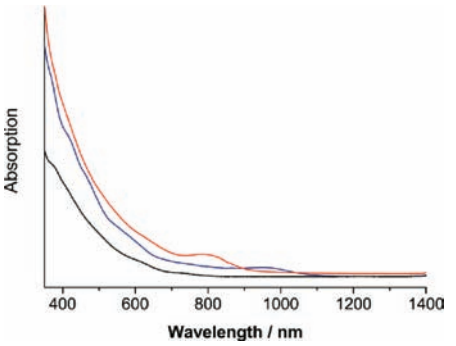

Figure 4. UV−vis−NIR spectra of $Sc_3N@I_h$-C_{80} (black), **1a** (blue), and **1b** (red) in toluene solution.

Spectroscopic Structure Determination of the Adducts. MALDI-TOF mass spectrum of the multiple adducts showed that the $Sc_3N@I_h$-C_{80} can be derivatized with up to 10 benzene addends (Figure 2a). **1a** exhibits a molecular ion peak at m/z 1185.163 and a peak at m/z 1108.871 due to the loss of the addend (Figure 2b). For **1b**, only the molecular ion peak at m/z 1185.229 was observed, not the parent $Sc_3N@I_h$-C_{80} (Figure 2c). On the basis of the mass values, both **1a** and **1b** are found to be the monoadducts of $Sc_3N@I_h$-C_{80}.

There are two types of ring junctions available on the I_h symmetric C_{80} cage. The 5,6-ring junction between one five- and one six-membered ring and the 6,6-ring junction occurs between two six-membered rings. The ^{1}H NMR spectrum of **1a** recorded in CS_2 solution is shown in Figure 3a. The spectrum displays two singlet signals at 7.43 and 7.23 ppm that integrate to a 1:1 ratio, which indicates only two types of phenyl protons on the benzene group and a symmetry plane in the adduct. The ^{1}H NMR spectrum of **1b** recorded in CS_2 solution (Figure 3b) exhibits three multiplet signals centered at 6.71, 6.66, and 6.62 ppm with the integration ratio of 2:1:1. Therefore, the addition pattern for **1b** must be unsymmetrical. Similar results have been reported by Dorn et al. for the *N*-tritylazomethine ylide symmetric and unsymmetric addition pattern on the $Sc_3N@I_h$-C_{80} cage.[27] On the basis of symmetry considerations, the observed NMR signals of **1a** are found to be consistent with a [5,6]-addition pattern and those of **1b** are consistent with a [6,6]-addition pattern. Thus, we assigned **1a** the 5,6-ring junction structure and **1b** the 6,6-ring junction adduct of $Sc_3N@I_h$-C_{80}. But whether the C−C bond at the site of addition on the fullerene is closed or open could not be determined from NMR measurements because the low solubility of the two samples precluded acquisition of ^{13}C NMR spectra.

The UV−vis−NIR spectra of both regioisomers along with the parent $Sc_3N@I_h$-C_{80} are shown in Figure 4. The spectrum of **1a** shows four weak absorptions centered at 422, 467, 580, and 955 nm, while **1b** only shows a strong and broad absorption centered at 800 nm, which is consistent with the results observed for the [6,6]-*N*-tritylpyrrolidino adduct of $Sc_3N@I_h$-C_{80}.[27] Both isomers show different absorptions from those of $Sc_3N@I_h$-C_{80}, which suggests that the electronic state of the C_{80} cage is altered by the cycloaddition of the benzyne group. Previous studies have shown that the UV−vis−NIR absorptions of [60]fullerene bisadducts are sensitive to the addition pattern rather than the nature of the addends,[46−48] therefore the UV−vis−NIR spectrum can be regarded as a powerful tool to determine the addition pattern of fullerene adducts. According to a previous report, the characteristic absorption behavior centered at 800 nm is associated with the [6,6]-regioaddition on the I_h C_{80} cage.[27] Thus, the UV−vis−NIR spectra are also consistent with **1b** being the [6,6]-regioisomer addition product and **1a** being the [5,6]-adduct.

Crystallographic Characterization of the Adducts. Diffusion of hexane into a carbon disulfide solution of each of the monoadducts produced black crystals of $Sc_3N@I_h$-C_{80}-(C_6H_4)-(5,6 isomer)·$2CS_2$ and $Sc_3N@I_h$-$C_{80}(C_6H_4)$-(6,6 isomer)·$2CS_2$ that were suitable for single-crystal X-ray diffraction. The structures of each adduct are shown in Figure 5.

For $Sc_3N@I_h$-$C_{80}(C_6H_4)$-(5,6 isomer)·$2CS_2$ the fullerene cage is disordered about a crystallographic mirror plane that contains C1, C5, and the benzyne adduct and bisects the C_{80} cage. This disorder interchanges the locations of the five- and six-membered rings that are attached to the benzyne unit and is typical disorder that is observed when additions occur at 5,6-ring junctions of fullerenes.[36,49] While the Sc_3N is disordered as well, there is only one sensible position (which is shown in Figure 5) for this group within a resolved cage orientation. The planar

dx.doi.org/10.1021/ja1097176 |*J. Am. Chem. Soc.* 2011, 133, 1563–1571

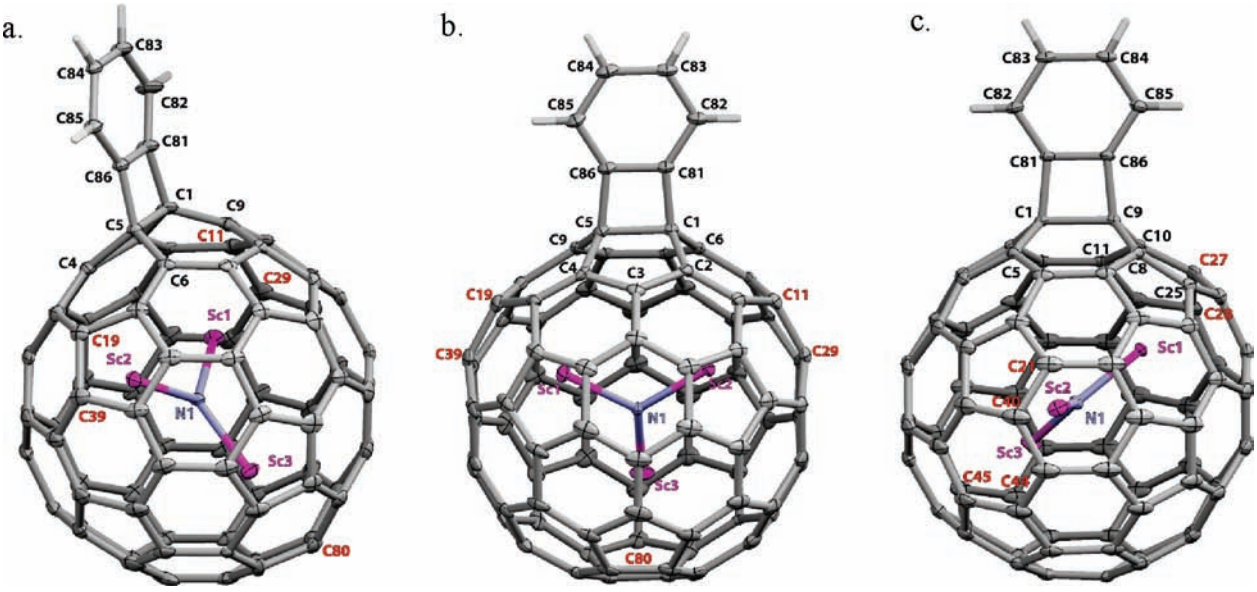

Figure 5. X-ray crystal structures of the [5,6]-benzyne monoadduct (shown in two perspectives a, b) in crystalline $Sc_3N@I_h$-$C_{80}(C_6H_4)\cdot 2CS_2$ ([5,6]-isomer) and [6,6]-benzyne monoadduct (c) in crystalline $Sc_3N@I_h$-$C_{80}(C_6H_4)\cdot 2CS_2$ ([6,6]-isomer) drawn with 50% thermal contours. Only the major orientations of the respective Sc_3N units are shown. The solvate molecules have been omitted for clarity. The carbon atoms closest to the scandium atoms are numbered in red.

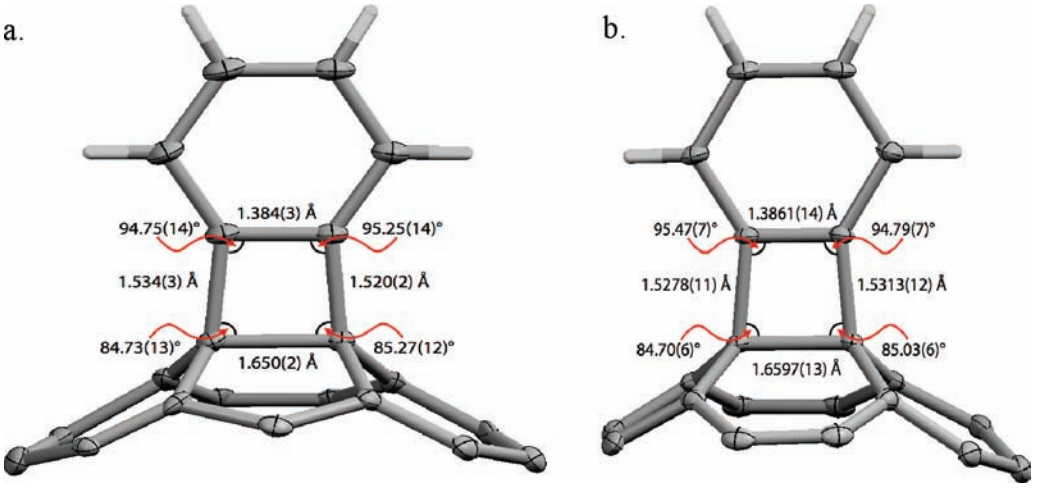

Figure 6. Portion of the [5,6]-benzyne monoadduct (a) and [6,6]-benzyne monoadduct (b) structures. This perspective highlights the [2 + 2] cycloaddition site as well as relevant bond distances and angles. All non-hydrogen atoms are drawn with 50% thermal contours.

Sc_3N unit is arranged so that the metal atoms avoid close interaction with the carbon atoms near the site of addition.

In $Sc_3N@I_h$-$C_{80}(C_6H_4)$-([6,6]-isomer)$\cdot 2CS_2$ the fullerene cage is fully ordered, but there is some disorder in the positions of the scandium atoms. The major orientation, which is shown in Figure 5, was modeled with the set Sc1, Sc2, and Sc3 with fractional occupancies of 0.90, 0.90, and 0.80, respectively. Again, the metal atoms, including the minor positions, are located so that they avoid close interaction with the carbon atoms at the site of addition.

Strauss, Boltalina, and co-workers have noted a preference for metal atoms in functionalized endohedral fullerenes to be located near carbon atoms in six-membered rings that are para to the sp^3 hybridized carbon atoms of the fullerene cage.[30] In agreement with their premise, in the [5,6]-isomer the scandium atoms are closest to carbon atoms in C−C bonds (C11−C29 and C19−C39) that are para to the sp^3 hybridized carbon atoms C1 and C5. The location of the scandium ions in the [6,6]-isomer is clearly different from that in the [5,6]-isomer. In the [6,6]-isomer the Y shape of the Sc_3N group does not straddle the site of addition. Rather, one scandium atom, Sc1, is located near C26, the carbon atom para to the sp^3 hybridized C9, and even nearer to C27, the carbon atom meta to C9.

The positioning of the scandium atoms near the cage surface causes an increase in the pyramidalization[50] of the adjacent carbon atoms, an effect noted in some other endohedral fullerenes.[51] The carbon atoms nearest the scandium atoms in these isomers show greater pyramidalization than carbons atoms further from these scandium atoms. Figures 7 and 8 show the pyramidalizations for the cage carbon atoms in the [5,6]-isomer and the [6,6]-isomer, respectively. The most pyramidalized carbon atoms are those at the site of addition as shown in the

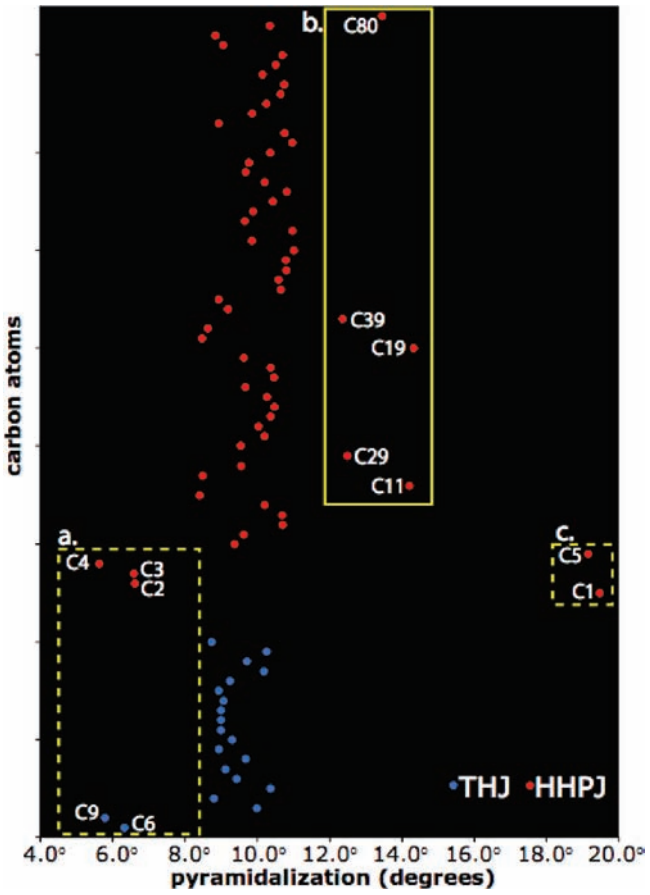

Figure 7. Pyramidalization of the carbon atoms in $Sc_3N@C_{80}$-$(C_6H_4)\cdot 2CS_2$ ([5,6]-isomer) as a function of carbon number with the carbon atoms at triple hexagon junctions (THJ) in blue at the bottom and carbon atoms at hexagon−hexagon−pentagon junctions (HHPJ) in red at the top. The yellow dashed box in (a) outlines the flattened carbon atoms that are adjacent to the addition site. The yellow box in (b) shows the carbon atoms closest to the scandium atoms. The yellow dashed box in (c) outlines the highly pyramidalized carbon atoms at the site of the benzyne addition.

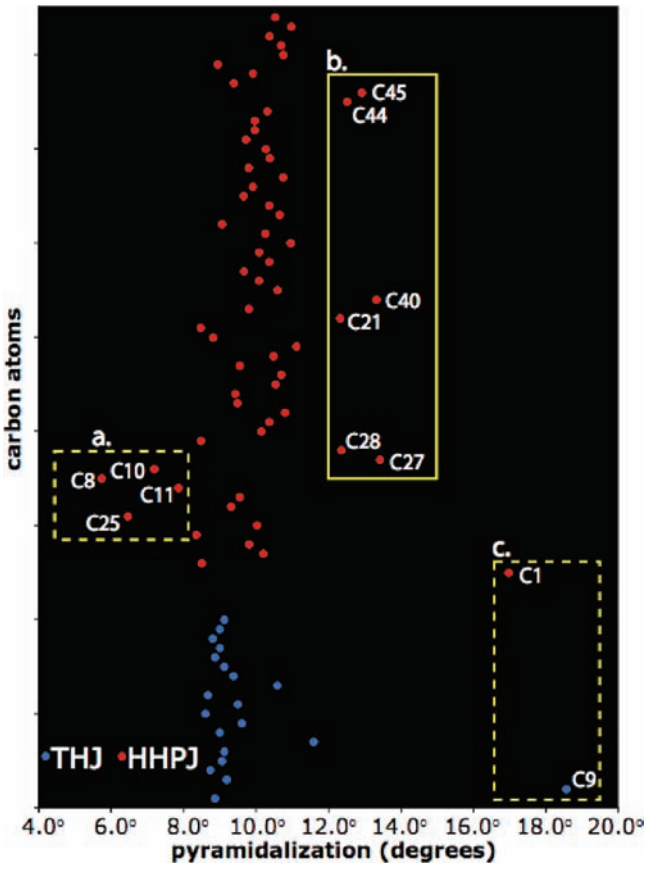

Figure 8. Pyramidalization of the carbon atoms in $Sc_3N@C_{80}$-$(C_6H_4)\cdot 2CS_2$ ([6,6]-isomer) as a function of carbon number with the carbon atoms at triple hexagon junctions (THJ) in blue at the bottom and carbon atoms at hexagon−hexagon−pentagon junctions (HHPJ) in red at the top. The yellow dashed box in (a) outlines the flattened carbon atoms that are adjacent to the addition site. The yellow box in (b) shows the carbon atoms closest to the scandium atoms. The yellow dashed box in (c) outlines the highly pyramidalized carbon atoms at the site of the benzyne addition.

yellow boxes labeled c in these figures. The next most pyramidalized sets of carbon atoms are those in the boxes labeled b, which are the carbon atoms nearest the scandium atoms. Note also that some of the carbon atoms in the rings immediately adjacent to the sites of addition show considerable flattening as seen in the boxes labeled c in the figures.

Figure 6 shows some structural details of the site of addition for the two adducts. The closed cyclobutenyl units are planar. The C1−C5 and C1−C9 bonds have undergone elongation, when compared to the typical C−C bond lengths, 1.437(15) Å and 1.421(18) Å, at 5,6- and 6,6-ring junctions in $Sc_3N@I_h$-C_{80}.[50] However, the C1−C5 and C1−C9 bond lengths, 1.650(2) and 1.6597(13) Å, respectively, in the two adducts are not much longer than the corresponding C−C distance, 1.645(8) Å, in the simple fullerene adduct $C_{60}C_6H_4$.[40]

Electrochemical Properties. Due to their high sensitivity and relatively low cost, electrochemical methods are very useful to provide valuable information about the electronic structures of low-yielding metallic nitride EMFs and their derivatives. On the basis of many reports, the electrochemical behavior of the monoadducts depends dramatically on the position of the addend.[4] It has been shown that [5,6]-TNT-EMF adducts exhibit reversible cathodic electrochemical behavior, while [6,6]-adducts exhibit irreversible behavior. 1,4-Adducts of $Sc_3N@C_{80}$ exhibit both reversible cathodic and anodic behavior,[30,52] therefore electrochemistry was suggested as a technique to determine the location of the functional groups on the cage surfaces.[23]

As shown in Figure 9 cyclic voltammetry (CV) of both the [5,6]- and [6,6]-regioisomers were performed and compared with that of the pristine fullerene compound in *o*-dichlorobenzene (*o*-DCB) containing 0.05 M tetra-*n*-butylammonium-hexafluorophosphate (n-Bu_4N)(PF_6) as the supporting electrolyte. This is the first report of the electrochemical behavior of a $Sc_3N@I_h$-C_{80} [6,6]-adduct. The electrochemical behavior of the [5,6]-regioisomer is similar to those of other reported TNT-EMFs [5,6]-monoadducts,[23] which display reversible cathodic electrochemical properties (Figure 9a). Three one-electron reversible reductions at −1.11, −1.50, and −2.21 V vs Fc/Fc^+ and two irreversible oxidations at +0.34 and +0.92 V vs Fc/Fc^+ were observed. Surprisingly, the [6,6]-derivative also exhibits electrochemically reversible cathodic and anodic behavior (Figure 9b). At a scan rate of 100 mV/s, three one-electron

dx.doi.org/10.1021/ja1097176 |*J. Am. Chem. Soc.* 2011, 133, 1563–1571

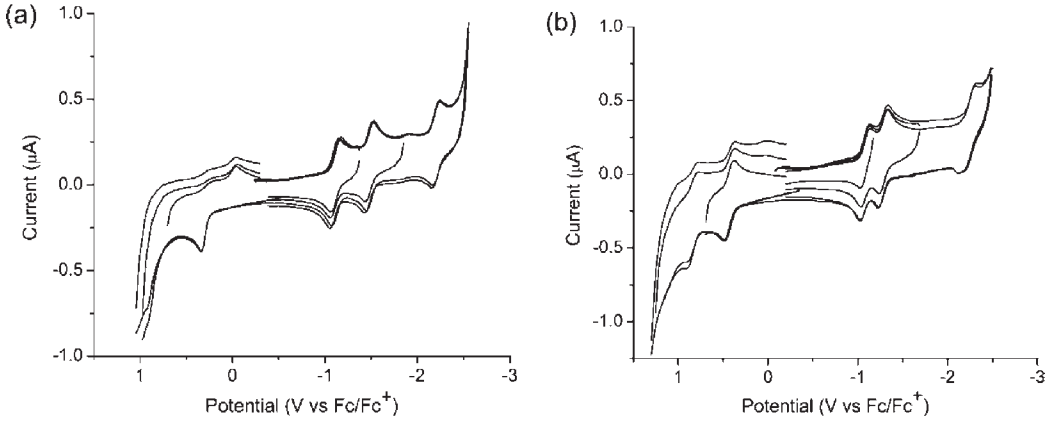

Figure 9. Cyclic voltammograms of (a) [5,6]-regioisomer and (b) [6,6]-regioisomer. The voltammograms were recorded in a 0.05 M solution of tetra-*n*-butylammonium-hexafluorophosphate in *o*-dichlorobenzene with a glassy carbon electrode as working electrode, silver wire as pseudoreference, and platinum wire as counter electrode with a scan rate of 100 mV/s.

Table 1. Redox Potentials of $Sc_3N@I_h$-C_{80} vs Fc/Fc^+

	$E^{+/2+}$ [V]	$E^{0/+}$ [V]	$E^{0/-}$ [V]	$E^{-/2-}$ [V]	$E^{2-/3-}$ [V]
$Sc_3N@I_h$-C_{80}[a]	+1.09[b]	+0.59[b]	−1.26	−1.62	−2.37
[5,6]-monoadduct	+0.92[c]	+0.34[c]	−1.11	−1.50	−2.21
[6,6]-monoadduct	+0.83[b]	+0.42	−1.08	−1.29	−2.23

[a] From ref 45. [b] Quasi-reversible process. [c] Irreversible process (reported values are peak potentials).

reversible reductions at −1.08, −1.29, and −2.23 V vs Fc/Fc^+ and one-electron reversible oxidation and one quasi-reversible oxidation were observed at +0.42 and +0.83 V vs Fc/Fc^+. This electrochemical behavior is different from those reported for the [6,6]-derivatives of $Y_3N@C_{80}$ and $Er_3N@C_{80}$, which display irreversible cathodic and anodic electrochemical properties.[23] However, the behavior is similar to that observed for the 1,4-trifluoromethylated bis-adduct of $Sc_3N@C_{80}$, $Sc_3N@C_{80}$-$(CF_3)_2$, which displays three reversible one-electron reductions and two reversible one-electron oxidations.[52] Table 1 compares the measured redox potentials of the pristine[45] and functionalized $Sc_3N@I_h$-C_{80}. The first reduction potentials of both [5,6]- and [6,6]-adducts are shifted to less negative potentials than that of the $Sc_3N@I_h$-C_{80}, indicating they have relatively low-lying LUMOs. Three reversible waves with potential spacing indicative of a nondegenerate LUMO and accessible LUMO+1 constitute the reductive voltammograms for both [5,6]- and [6,6]-adducts. The first and second reduction potentials for the [6,6]-isomer are very close to each other, and the separation between the second and the third is larger. This electrochemical behavior is very similar to that of $Yb@C_{84}$.[53] This is the first example of electrochemically reversible behavior for a [6,6]-derivative of $Sc_3N@I_h$-C_{80}. So far, this behavior is exclusive for the $Sc_3N@I_h$-C_{80} [6,6]-adducts, and the reason is not well understood.

Thermal Stability of the [5,6]- and [6,6]-Regioisomers. In view of the promising applications of endohedral metallofullerene derivatives, exploring new ways to functionalize TNT-EMFs, especially the formation of highly stable derivatives is crucial for expanding their applications. As is well-known, many organofullerenes are not stable and undergo retro-addition reactions or isomerizations under reductive,[54−59] oxidative,[60] or high temperature conditions.[61−64] Recently the retro-addition reaction

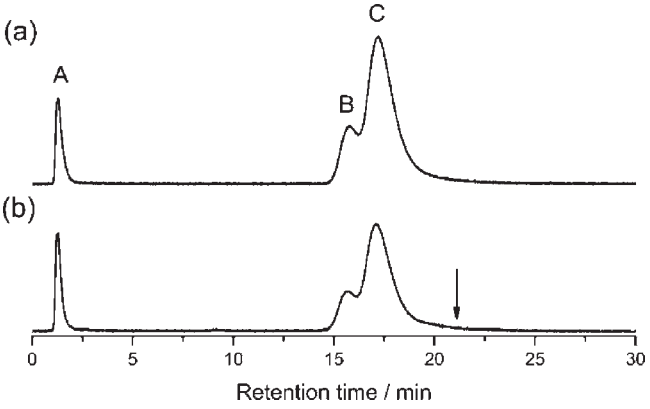

Figure 10. HPLC chromatograms of a mixture for the [5,6]-regioisomer (C) and [6,6]-regioisomer (B) of $Sc_3N@I_h$-C_{80} at times (a) 0 h, (b) after 4 h in refluxing *o*-DCB at 180 °C. The peak labeled as A is *o*-DCB, and the arrow marks the retention time at which $Sc_3N@I_h$-C_{80} would elute if present. HPLC conditions: PBB column at 3.0 mL/min flow rate with toluene.

and isomerization occurring on the surface of endohedral metallofullerenes were reported. In 2006, Martín and Echegoyen[60] first reported the retrocycloaddition reaction of pyrrolidine derivatives of $Sc_3N@I_h$-C_{80} under thermal conditions. In the same year, Gibson and Dorn[27] observed the interconversion of *N*-tritylpyrrolidino [6,6]-monoadduct of $Sc_3N@I_h$-C_{80} into the corresponding thermodynamically more stable [5,6]-monoadduct. In 2007, Wang and co-workers[25] described the thermal stabilities of $Sc_xGd_{3-x}N@C_{80}$ (x = 0−3) pyrrolidine monoadducts and the size effect of endohedral clusters on the isomerization between [5,6]- and [6,6]-regioisomers. So far, most of the pyrrolidine derviatives of TNT-EMFs are unstable at elevated temperatures. The benzyne cycloaddition derivatives of $Sc_3N@I_h$-C_{80} at both 5,6- and 6,6-ring junctions show significantly enhanced thermal stabilities relative to those of the pyrrolidine adducts. An *o*-dichlorobenzene solution of mixed [5,6]- and [6,6]-adducts was heated at reflux for 4 h; the composition of the solution was monitored via HPLC. The results of this study are shown in Figure 10. Both adducts remain stable even after heating to 180 °C for 4 h. No retro-addition reaction or interconversion was observed under these conditions which result in thermal

retro-addition or isomerization in the case of pyrrolidine adducts. These stabilities persist in the presence of oxygen. The thermal stabilities of the isolated [5,6]- and [6,6]-isomers were also studied separately in refluxing *o*-DCB for 4 h or even more than 4 h. Product compositions were monitored via HPLC using either a Buckyclutcher or a PBB column, respectively. Only the starting isomers were recovered, and no decomposition or isomerization was observed. These exceptionally stable [2 + 2] cycloaddition adducts of $Sc_3N@I_h$-C_{80} are being further functionalized to pursue potential applications.

CONCLUSION

In summary, the first examples of [2 + 2] cycloaddition products of $Sc_3N@I_h$-C_{80} were reported. Both [5,6]- and [6,6]-monoadducts were synthesized, isolated, and fully characterized. This is the second example of $Sc_3N@I_h$-C_{80} that yields both [5,6]- and [6,6]-isomers in one reaction. Structurally, the two isomeric adducts contain closed, planar, cyclobutenyl units in which the fullerene C−C bond is elongated but not broken. The metal atoms inside each adduct assume positions that avoid close interaction with the carbon atoms near the site of addition. However, as seen in Figure 5, the positioning of the Sc_3N unit with regard to the location of the addend differs in the two isomers. Most interestingly, this is the first time the electrochemical properties of a $Sc_3N@I_h$-C_{80} [6,6]-monoadduct were observed, and it exhibits an unexpected electrochemically reversible cathodic behavior. Thermalization experiments showed that both monoadducts are very stable at relatively high temperatures. These findings may shed light on the design and synthesis of functionalized fullerenes with high stabilities for potential applications in photovoltaic devices.

EXPERIMENTAL SECTION

Materials and Methods. High-purity graphite rods (6-mm diameter; purchased from POCO) were core-drilled (4-mm diameter) and packed with graphite powder, scandium oxide, and copper with the weight ratio of $C/Sc_2O_3/Cu$ equal to 7/2/1. The I_h isomer of $Sc_3N@C_{80}$ was obtained according to the procedures as described in the Results and Discussion. Isoamyl nitrite, anthranilic acid, *o*-DCB, and toluene were used as received. Tetra-*n*-butylammonium-hexafluorophosphate (n-Bu_4N)(PF_6) was recrystallized from absolute ethanol and dried in vacuum before use. The purity of the compounds was verified by HPLC by using a Varian Prostar 210 equipped with a PBB (4.5 mm × 250 mm) and/or a Buckyprep column (10 mm × 250 mm) and toluene as eluent with a flow rate of 2 mL/min and 4 mL/min, respectively. MALDI-TOF mass spectrometry was carried out on a Voyager-DE STR mass spectrometer. The NMR spectra were recorded by using a 500 MHz Bruker spectrometer instrument. The UV−vis−NIR spectra were taken using a Perkin-Elmer Lambda 950 spectrophotometer. Cyclic voltammetry was carried out in a one-compartment cell connected to a BAS 100B workstation in a solution of *o*-DCB containing 0.05 M (n-Bu_4N)(PF_6). A 2-mm diameter glassy carbon disk was used as the working electrode. Ferrocene was added to the solution at the end of each experiment as an internal standard.

Synthesis of 1a and 1b. Typically (Scheme 1), 5 mL of *o*-dichlorobenzene and 20 mL of toluene solution containing 4 mg of $Sc_3N@I_h$-C_{80} (0.004 mmol) was bubbled with argon for 10 min, and 7.3 μL (0.05 mmol) of isoamyl nitrite was added with argon bubbling for another 10 min; then 7.4 mg (0.05 mmol) of anthranilic acid was added. After stirring under argon for 3 h at room temperature, the solvent was removed, and the residue was washed with methanol to remove the starting materials before further purification with HPLC. **1a** and **1b** were isolated with the respective yields of 70% and 15% based on consumed $Sc_3N@I_h$-C_{80} as black solids from the reaction mixtures and purified through two HPLC stages with toluene as solvent. **1a**: ^{1}H NMR (500 MHz, CS_2/CD_3OCD_3, 25 °C, TMS): δ = 7.43 (s, 2H; Ph-H), 7.23 (s, 2H; Ph-H); UV−vis−NIR (toluene): λ = 422, 467, 580, and 955 nm; MALDI-TOF-MS: (positive ionization mode 9-nitroanthracene as matrix): m/z: 1185.163; **1b**: ^{1}H NMR (500 MHz, CS_2/CD_3OCD_3, 25 °C, TMS): δ = 6.71 (m, 2H; Ph-H), 6.66 (m, 1H; Ph-H), 6.62, (m, 1H; Ph-H); UV−vis−NIR (toluene): λ = 800 nm; MALDI-TOF-MS: (positive ionization mode 9-nitroanthracene as matrix): m/z: 1185.229.

X-ray Crystallography and Data Collection of $Sc_3N@I_h$-$C_{80}(C_6H_4)$-(5,6-isomer)·$2CS_2$. Black parallelepipeds were obtained by diffusion of hexane into a carbon disulfide solution of the monoadduct. A crystal of dimensions 0.33 mm × 0.17 mm × 0.12 mm was mounted in the 100(2) K nitrogen cold stream provided by an Oxford Cryostream low-temperature apparatus on the goniometer head of a Bruker D8 diffractometer equipped with an ApexII CCD detector of beamline 11.3.1 at the Advanced Light Source in Berkeley, CA. Diffraction data were collected using synchrotron radiation monochromated with silicon(111) to a wavelength of 0.77490 Å. An approximate full sphere of data to 2θ = 81.4° was collected using 0.3° ω scans. A multiscan absorption correction was applied using the program SADABS-2008/1. A total of 90812 reflections was collected, of which 10896 were unique [R(int) = 0.0509] and 9978 were observed [$I > 2\sigma(I)$]. The structure was solved by direct methods (SHELXS) and refined by full-matrix least-squares on F^2 (SHELXL97) using 793 parameters and 0 restraints.

The hydrogen atoms were generated geometrically and refined as riding atoms with C−H distances = 0.95 Å and U_{iso}(H) = 1.2 times U_{eq}(C). The maximum and minimum peaks in the final difference Fourier map were 1.565 and −1.262 eÅ^{-3}.

Crystal data: $C_{88}H_4NS_4Sc_3$, M_w = 1338.04 amu, orthorhombic, *Pnma*, a = 19.6998(6) Å, b = 14.7348(5) Å, c = 15.5859(5) Å, V = 4524.2(3) Å^3, T = 100(2) K, Z = 4, R_1 [$I > 2\sigma(I)$] = 0.0662, wR_2 (all data) = 0.2011, GOF (on F^2) = 1.052.

X-ray Crystallography and Data Collection of $Sc_3N@I_h$-$C_{80}(C_6H_4)$-(6,6-isomer)·$2CS_2$. Black plates were obtained by diffusion of hexane into a carbon disulfide solution of the monoadduct. A crystal with dimensions 0.17 mm × 0.11 mm × 0.05 mm was mounted on beamline 11.3.1 at the Advanced Light Source in Berkeley, CA as described above. Diffraction data were collected using synchrotron radiation monochromated with silicon(111) to a wavelength of 0.77490 Å. An approximate full sphere of data to 2θ = 101.6° was collected using 0.3° ω scans. A multiscan absorption correction was applied using the program SADABS-2008/1. A total of 216696 reflections was collected, of which 37767 were unique [R(int) = 0.0463] and 36408 were observed [$I > 2\sigma(I)$]. The structure was solved by direct methods (SHELXS) and refined by full-matrix least-squares on F^2 (SHELXL97) using 918 parameters and 0 restraints. The structure was refined as a racemic twin.

The hydrogen atoms were treated as described previously. The maximum and minimum peaks in the final difference Fourier map were 2.49 and −0.77 eÅ^{-3}.

Crystal data: $C_{88}H_4NS_4Sc_3$, M_w = 1338.04 amu, orthorhombic, $P2_12_12_1$, a = 14.7764(4) Å, b = 15.6777(5) Å, c = 19.5438(6) Å, V = 4527.5(2) Å^3, T = 100(2) K, Z = 4, R_1 [$I > 2\sigma(I)$] = 0.0550, wR_2 (all data) = 0.1523, GOF (on F^2) = 1.066.

ASSOCIATED CONTENT

Supporting Information. Complete ref 5. X-ray crystallographic files in CIF format for $Sc_3N@I_h$-$C_{80}(C_6H_4)$-(5,6 isomer)·$2CS_2$ and $Sc_3N@I_h$-$C_{80}(C_6H_4)$-(6,6 isomer)·$2CS_2$.

This material is available free of charge via the Internet at http://pubs.acs.org.

AUTHOR INFORMATION

Corresponding Author
echegoyen@utep.edu; albalch@ucdavis.edu; mmolmstead@ucdavis.edu

ACKNOWLEDGMENT

Financial support from the National Science Foundation (Grant DMR-0809129 to F.L., J.P., and L.E.) is greatly appreciated. We also thank the National Science Foundation (Grant CHE-1011760 to A.L.B. and M.M.O.) and the Advanced Light Source, supported by the Director, Office of Science, Office of Basic Energy Sciences, of the U.S. Department of Energy under Contract No. DE-AC02-05CH11231, for beam time, and Dr. Simon J. Teat and Dr. Christine M. Beavers for their assistance.

REFERENCES

(1) Stevenson, S.; Rice, G.; Glass, T.; Harich, K.; Cromer, F.; Jordan, M. R.; Craft, J.; Hadju, E.; Bible, R.; Olmstead, M. M.; Maitra, K.; Fisher, A. J.; Balch, A. L.; Dorn, H. C. *Nature* **1999,** *401*, 55–57.

(2) Stevenson, S.; Fowler, P. W.; Heine, T.; Duchamp, J. C.; Rice, G.; Glass, T.; Harich, K.; Hajdu, E.; Bible, R.; Dorn, H. C. *Nature* **2000,** *408*, 427–428.

(3) Dunsch, L.; Yang, S. F. *Small* **2007,** *3*, 1298–1320.

(4) Chaur, M. N.; Melin, F.; Ortiz, A. L.; Echegoyen, L. *Angew. Chem., Int. Ed.* **2009,** *48*, 7514–7538.

(5) Zhang, J. F.; et al. *Nano Lett.* **2010,** *10*, 2843–2848.

(6) Shultz, M. D.; Duchamp, J. C.; Wilson, J. D.; Shu, C. Y.; Ge, J.; Zhang, J.; Gibson, H. W.; Fillmore, H. L.; Hirsch, J. I.; Dorn, H. C.; Fatouros, P. P. *J. Am. Chem. Soc.* **2010,** *132*, 4980–4981.

(7) Zhang, E. Y.; Shu, C. Y.; Feng, L.; Wang, C. R. *J. Phys. Chem. B* **2007,** *111*, 14223–14226.

(8) Bolskar, R. D. *Nanomedicine* **2008,** *3*, 201–213.

(9) Iezzi, E. B.; Duchamp, J. C.; Fletcher, K. R.; Glass, T. E.; Dorn, H. C. *Nano Lett.* **2002,** *2*, 1187–1190.

(10) Braun, K.; Dunsch, L.; Pipkorn, R.; Bock, M.; Baeuerle, T.; Yang, S.; Waldeck, W.; Wiessler, M. *Int. J. Med. Sci.* **2010,** *7*, 136–146.

(11) Pinzón, J. R.; Plonska-Brzezinska, M. E.; Cardona, C. M.; Athans, A. J.; Gayathri, S. S.; Guldi, D. M.; Herranz, M. A.; Martín, N.; Torres, T.; Echegoyen, L. *Angew. Chem., Int. Ed.* **2008,** *47*, 4173–4176.

(12) Pinzón, J. R.; Cardona, C. M.; Herranz, M. A.; Plonska-Brzezinska, M. E.; Palkar, A.; Athans, A. J.; Martín, N.; Rodríguez-Fortea, A.; Poblet, J. M.; Bottari, G.; Torres, T.; Gayathri, S. S.; Guldi, D. M.; Echegoyen, L. *Chem.—Eur. J.* **2009,** *15*, 864–877.

(13) Pinzón, J. R.; Gasca, D. C.; Sankaranarayanan, S. G.; Bottari, G.; Torres, T.; Guldi, D. M.; Echegoyen, L. *J. Am. Chem. Soc.* **2009,** *131*, 7727–7734.

(14) Shu, C. Y.; Xu, W.; Slebodnick, C.; Champion, H.; Fu, W. J.; Reid, J. E.; Azurmendi, H.; Wang, C. R.; Harich, K.; Dorn, H. C.; Gibson, H. W. *Org. Lett.* **2009,** *11*, 1753–1756.

(15) Ross, R. B.; Cardona, C. M.; Guldi, D. M.; Sankaranarayanan, S. G.; Reese, M. O.; Kopidakis, N.; Peet, J.; Walker, B.; Bazan, G. C.; Van Keuren, E.; Holloway, B. C.; Drees, M. *Nat. Mater.* **2009,** *8*, 208–212.

(16) Ross, R. B.; Cardona, C. M.; Swain, F. B.; Guldi, D. M.; Sankaranarayanan, S. G.; Van Keuren, E.; Holloway, B. C.; Drees, M. *Adv. Funct. Mater.* **2009,** *19*, 2332–2337.

(17) Iezzi, E. B.; Duchamp, J. C.; Harich, K.; Glass, T. E.; Lee, H. M.; Olmstead, M. M.; Balch, A. L.; Dorn, H. C. *J. Am. Chem. Soc.* **2002,** *124*, 524–525.

(18) Lee, H. M.; Olmstead, M. M.; Iezzi, E.; Duchamp, J. C.; Dorn, H. C.; Balch, A. L. *J. Am. Chem. Soc.* **2002,** *124*, 3494–3495.

(19) Maggini, M.; Scorrano, G.; Prato, M. *J. Am. Chem. Soc.* **1993,** *115*, 9798–9799.

(20) Cardona, C. M.; Kitaygorodskiy, A.; Ortiz, A.; Herranz, M. A.; Echegoyen, L. *J. Org. Chem.* **2005,** *70*, 5092–5097.

(21) Cai, T.; Ge, Z. X.; Iezzi, E. B.; Glass, T. E.; Harich, K.; Gibson, H. W.; Dorn, H. C. *Chem. Commun.* **2005,** 3594–3596.

(22) Cardona, C. M.; Kitaygorodskiy, A.; Echegoyen, L. *J. Am. Chem. Soc.* **2005,** *127*, 10448–10453.

(23) Cardona, C. M.; Elliott, B.; Echegoyen, L. *J. Am. Chem. Soc.* **2006,** *128*, 6480–6485.

(24) Campanera, J. M.; Bo, C.; Poblet, J. M. *J. Org. Chem.* **2006,** *71*, 46–54.

(25) Chen, N.; Zhang, E. Y.; Tan, K.; Wang, C. R.; Lu, X. *Org. Lett.* **2007,** *9*, 2011–2013.

(26) Chen, N.; Fan, L. Z.; Tan, K.; Wu, Y. Q.; Shu, C. Y.; Lu, X.; Wang, C. R. *J. Phys. Chem. C* **2007,** *111*, 11823–11828.

(27) Cai, T.; Slebodnick, C.; Xu, L.; Harich, K.; Glass, T. E.; Chancellor, C.; Fettinger, J. C.; Olmstead, M. M.; Balch, A. L.; Gibson, H. W.; Dorn, H. C. *J. Am. Chem. Soc.* **2006,** *128*, 6486–6492.

(28) Iiduka, Y.; Ikenaga, O.; Sakuraba, A.; Wakahara, T.; Tsuchiya, T.; Maeda, Y.; Nakahodo, T.; Akasaka, T.; Kako, M.; Mizorogi, N.; Nagase, S. *J. Am. Chem. Soc.* **2005,** *127*, 9956–9957.

(29) Wakahara, T.; Iiduka, Y.; Ikenaga, O.; Nakahodo, T.; Sakuraba, A.; Tsuchiya, T.; Maeda, Y.; Kako, M.; Akasaka, T.; Yoza, K.; Horn, E.; Mizorogi, N.; Nagase, S. *J. Am. Chem. Soc.* **2006,** *128*, 9919–9925.

(30) Shustova, N. B.; Popov, A. A.; Mackey, M. A.; Coumbe, C. E.; Phillips, J. P.; Stevenson, S.; Strauss, S. H.; Boltalina, O. V. *J. Am. Chem. Soc.* **2007,** *129*, 11676–11677.

(31) Shu, C. Y.; Slebodnick, C.; Xu, L. S.; Champion, H.; Fuhrer, T.; Cai, T.; Reid, J. E.; Fu, W. J.; Harich, K.; Dorn, H. C.; Gibson, H. W. *J. Am. Chem. Soc.* **2008,** *130*, 17755–17760.

(32) Bingel, C. *Chem. Ber.* **1993,** *126*, 1957–1959.

(33) Hirsch, A.; Lamparth, I.; Groesser, T.; Karfunkel, H. R. *J. Am. Chem. Soc.* **1994,** *116*, 9385–9386.

(34) Shu, C. Y.; Cai, T.; Xu, L. S.; Zuo, T. M.; Reid, J.; Harich, K.; Dorn, H. C.; Gibson, H. W. *J. Am. Chem. Soc.* **2007,** *129*, 15710–15717.

(35) Pinzón, J. R.; Zuo, T.; Echegoyen, L. *Chem.—Eur. J.* **2010,** *16*, 4864–4869.

(36) Lukoyanova, O.; Cardona, C. M.; Rivera, J.; Lugo-Morales, L. Z.; Chancellor, C. J.; Olmstead, M. M.; Rodriguez-Fortea, A.; Poblet, J. M.; Balch, A. L.; Echegoyen, L. *J. Am. Chem. Soc.* **2007,** *129*, 10423–10430.

(37) Chaur, M. N.; Melin, F.; Athans, A. J.; Elliott, B.; Walker, K.; Holloway, B. C.; Echegoyen, L. *Chem. Commun.* **2008,** 2665–2667.

(38) Hoke, S. H., II; Molstad, J.; Dilettato, D.; Jay, M. J.; Carlson, D.; Kahr, B.; Cooks, R. G. *J. Org. Chem.* **1992,** *57*, 5069–5071.

(39) Tsuda, M.; Ishida, T.; Nogami, T.; Kurono, S.; Ohashi, M. *Chem. Lett.* **1992,** *21*, 2333–2334.

(40) Ishida, T.; Shinozuka, K.; Nogami, T.; Sasaki, S.; Iyoda, M. *Chem. Lett.* **1995,** *24*, 317–318.

(41) Meier, M. S.; Wang, G.-W.; Haddon, R. C.; Brock, C. P; Lloyd, M. A.; Selegue, J. P. *J. Am. Chem. Soc.* **1998,** *120*, 2337–2342.

(42) Lu, X.; Xu, J. X.; He, X. R.; Shi, Z. J.; Gu, Z. N. *Chem. Mater.* **2004,** *16*, 953–955.

(43) Lu, X.; Nikawa, H.; Tsuchiya, T.; Akasaka, T.; Toki, M.; Sawa, H.; Mizorogi, N.; Nagase, S. *Angew. Chem., Int. Ed.* **2010,** *49*, 594–597.

(44) Stevenson, S.; Mackey, M. A.; Thompson, M. C.; Coumbe, H. L.; Madasu, P. K.; Coumbe, C. E.; Phillips, J. P. *Chem. Commun.* **2007,** 4263–4265.

(45) Elliott, B.; Yu, L.; Echegoyen, L. *J. Am. Chem. Soc.* **2005,** *127*, 10885–10888.

(46) Djojo, F.; Herzog, A.; Lamparth, I.; Hampel, F.; Hirsch, A. *Chem.—Eur. J.* **1996,** *2*, 1537–1547.

(47) Nakamura, Y.; Takano, N.; Nishimura, T.; Yashima, E.; Sato, M.; Kudo, T.; Nishimura, J. *Org. Lett.* **2001,** *3*, 1193–1196.

(48) Kordatos, K.; Bosi, S.; Da Ros, T.; Zambon, A.; Lucchini, V.; Prato, M. *J. Org. Chem.* **2001,** *66*, 2802–2808.

(49) Miller, G. P.; Tetreau, M. C.; Olmstead, M. M.; Lord, P. A.; Balch, A. L. *Chem. Commun* **2001,** 1758–1759.

(50) Haddon, R. C.; Raghavachari, K. In *Buckminsterfullerenes*; Billups, W. E.; Ciufolini, M. A., Eds.; VCH: New York, 1993; Chaper 7, p 185.
(51) Lee, H. M.; Olmstead, M. M.; Iezzi, E.; Duchamp, J. C.; Dorn, H. C.; Balch, A. L. *J. Am. Chem. Soc.* **2002,** *124,* 3494–3495.
(52) Popov, A. A.; Shustova, N. B.; Svitova, A. L.; Mackey, M. A.; Coumbe, C. E.; Phillips, J. P.; Stevenson, S.; Strauss, S. H.; Boltalina, O. V.; Dunsch, L. *Chem.—Eur. J.* **2010,** *16,* 4721–4724.
(53) Lu, X.; Slanina, Z.; Akasaka, T.; Tsuchiya, T.; Mizorogi, N.; Nagase, S. *J. Am. Chem. Soc.* **2010,** *132,* 5896–5905.
(54) Kessinger, R.; Crassous, J.; Herrmann, A.; Rüttimann, M.; Echegoyen, L.; Diederich, F. *Angew. Chem., Int. Ed.* **1998,** *37,* 1919–1922.
(55) Crassous, J.; Rivera, J.; Fender, N. S.; Shu, L.; Echegoyen, L.; Thilgen, C.; Herrmann, A.; Diederich, F. *Angew. Chem., Int. Ed.* **1999,** *38,* 1613–1617.
(56) Moonen, N. N. P.; Thilgen, C.; Echegoyen, L.; Diederich, F. *Chem. Commun.* **2000,** 335–336.
(57) Beulen, M. W. J.; Rivera, J. A.; Herranz, M. Á.; Illescas, B.; Martín, N.; Echegoyen, L. *J. Org. Chem.* **2001,** *66,* 4393–4398.
(58) Herranz, M. Á.; Beulen, M. W. J.; Rivera, J. A.; Echegoyen, L.; Díaz, M, C.; Illescas, B.; Martín, N. *J. Mater. Chem.* **2002,** *12,* 2048–2053.
(59) Herranz, M. Á.; Cox, C. T., Jr.; Echegoyen, L. *J. Org. Chem.* **2003,** *68,* 5009–5012.
(60) Lukoyanova, O.; Cardona, C. M.; Altable, M.; Filippone, S.; Domenech, Á. M.; Martín, N.; Echegoyen, L. *Angew. Chem., Int. Ed.* **2006,** *45,* 7430–7433.
(61) Martín, N.; Altable, M.; Filippone, S.; Martín-Domenech, A.; Echegoyen, L.; Cardona, C. M. *Angew. Chem., Int. Ed.* **2005,** *45,* 110–114.
(62) Martín, N.; Altable, M.; Filippone, S.; Martín-Domenech, A.; Martínez-Álvarez, R.; Suarez, M.; Plonska-Brzezinska, M. E.; Lukoyanova, O.; Echegoyen, L. *J. Org. Chem.* **2007,** *72,* 3840–3846.
(63) Delgado, J. L.; Oswald, F.; Cardinali, F.; Langa, F.; Martín, N. *J. Org. Chem.* **2008,** *73,* 3184–3188.
(64) Filippone, S.; Barroso, M. I.; Martín-Domenech, Á.; Osuna, S.; Solà, M.; Martín, N. *Chem.—Eur. J.* **2008,** *14,* 5198–5206.